Electronic Supplementary Information

Wurtzite CoO: a direct band gap oxide suitable for photovoltaic absorber

Y. Wang[a,b,*], H.X. Ge[c], Y.P. Chen[c], X.Y. Meng[d], J. Ghanbaja[b], D. Horwat[b], J.F. Pierson[b]

[a] State Key Laboratory for Environmental-friendly Energy Materials, Southwest University of Science and Technology, Mianyang 621010, China.

[b] Institut Jean Lamour, UMR 7198-CNRS, Université de Lorraine, Nancy F-54011, France.

[c] School of Physics and Optoelectronics, Xiangtan University, Xiangtan 411105, China.

[d] Center for Green Research on Energy and Environmental Materials, National Institute for Materials Science, Tsukuba 305-0047, Japan.

[*]Corresponding author: Y. Wang Email: wangyongvlsi@hotmail.com

1. Cross-section microstructure of wurtzite CoO thin films

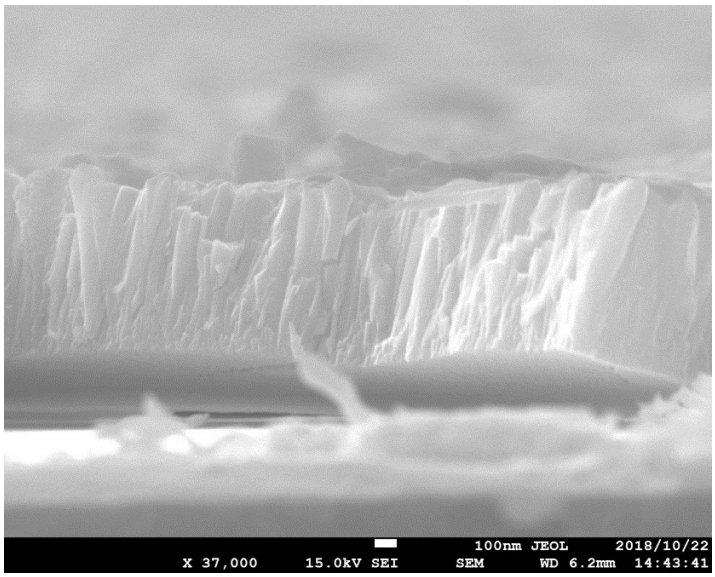

Fig. S1 Cross-section SEM image of wurtzite CoO thin film

The cross-section SEM image of wurtzite CoO thin film is presented in Fig. S1, which shows the dense columns along the film thickness direction. Here it is worth noting that the tilt columns in Fig. S1 are due to the upwarping SEM specimen, rather than the existence of tilt angle between columns and substrate normal.

2. Optical properties of wurtzite CoO thin films

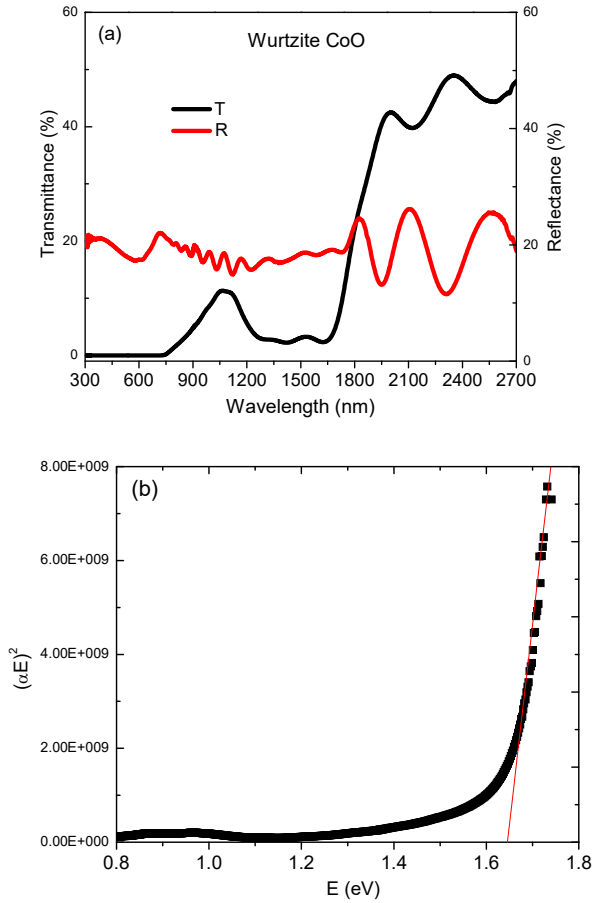

Fig. S2 (a) T and R of wurtzite CoO thin film. (b) Tauc fitting of $(\alpha E)^2$ vs. E for wurtzite CoO thin film.

The optical transmittance (T) and reflectance (R) of wurtzite CoO thin film is shown in Fig. S2. Using the formula $\alpha = -In(T/(1-R)^2)/d$ (where d is the thickness), the absorption coefficient (α) is calculated. Then the Tauc fitting of $(\alpha E)^2$ vs. E curve of the wurtzite CoO thin film is performed, as shown in Fig. S2(b), giving rise to a direct band gap of 1.64 eV.

3. PDOS in wurtzite CoO

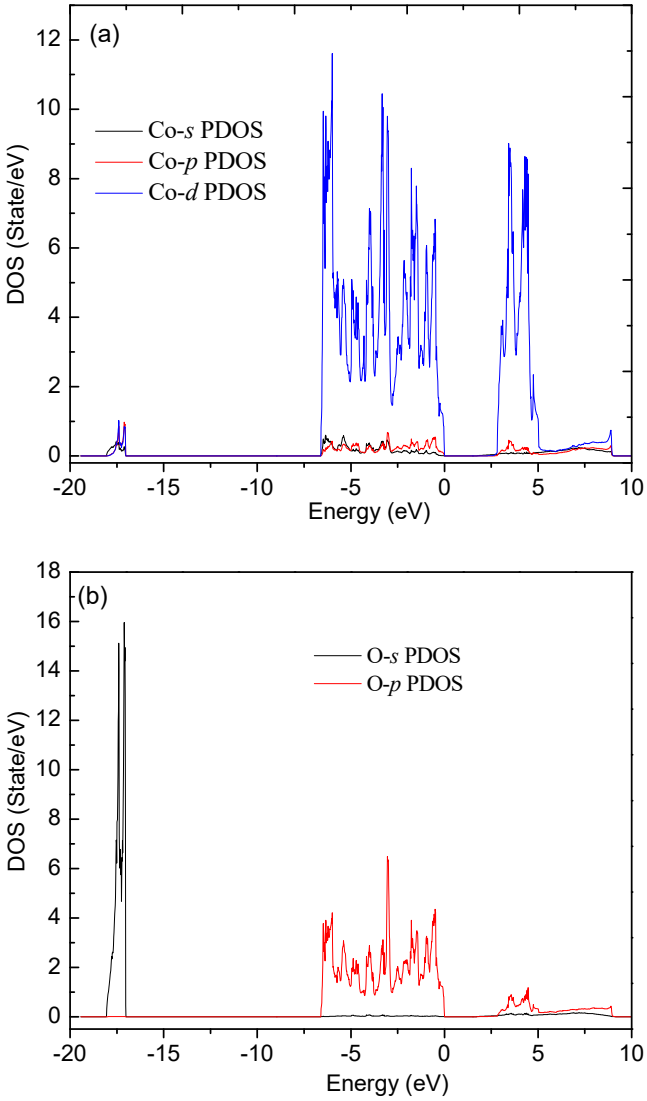

Fig. S3 (a) Co-*s*, Co-*p* and Co-*d* PDOS. (b) O-*s* and O-*p* PDOS. The energy zero is set at VBM.

The comparison of Co-*s*, Co-*p* and Co-*d* partial density of states (PDOS) of wurtzite CoO is shown in Fig. S3(a). The energy zero is set at valence band maximum (VBM). It is seen that Co-*d* PDOS is much stronger than Co-*s* and Co-*p* PDOS in the whole energy range. The comparison of O-*s* and O-*p* PDOS is present in Fig. S3(b), which indicates that O-*p* orbitals make predominant contributions in the energy range of -15 eV to 10 eV.

4. Phase structure identifications of rocksalt CoO and spinel Co_3O_4 thin films

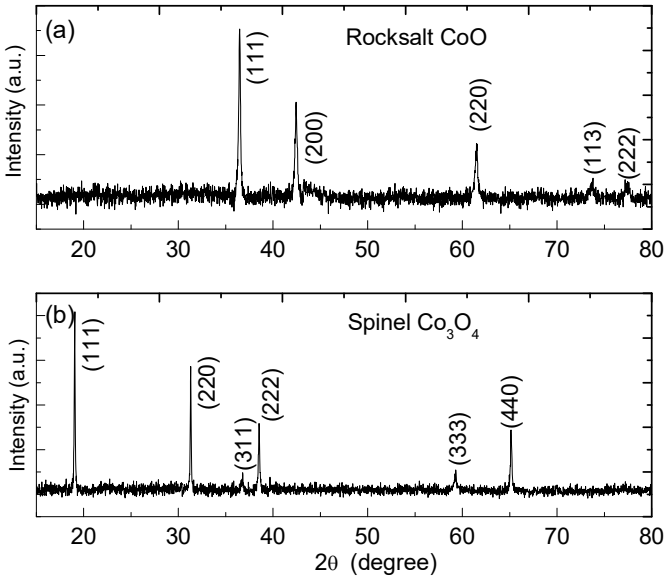

Fig. S4 X-ray diffractograms of rocksalt-type cubic CoO and spinel cubic Co_3O_4 thin films.

Fig. S4(a) and (b) show the X-ray diffractograms of thin films crystallize in rocksalt-type cubic CoO (JCPDS 04-001-8626) and spinel cubic Co_3O_4 (JCPDS 04-008-2376), respectively.

5. Microstructure of rocksalt CoO, wurtzite CoO and spinel Co_3O_4 thin films

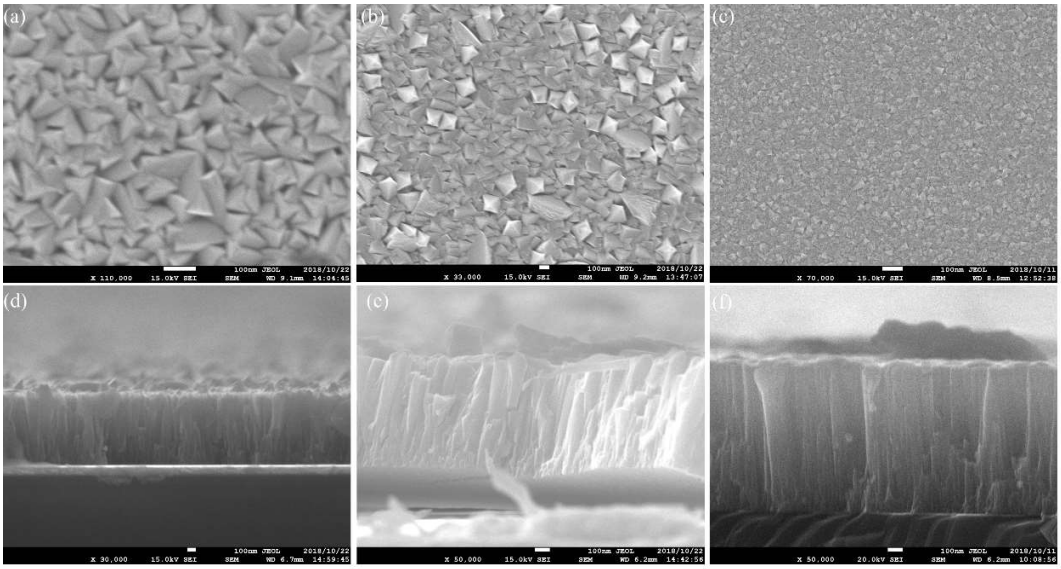

Fig. S5 (a), (b) and (c) are the top-view SEM images of rocksalt CoO, wurtzite CoO, and spinel Co_3O_4 thin films, respectively. (d), (e) and (f) are their corresponding cross-section images.

The top-view and cross-section SEM images of rocksalt CoO, wurtzite CoO, and spinel Co_3O_4 thin films are presented in Fig. S5 for a comparison. The top-view SEM images demonstrate the smooth surface and dense microstructure in these three phases. In addition, it is seen that all the thin films possess the columnar growth along the thickness direction.

6. Optical absorption of rocksalt CoO, wurtzite CoO and spinel Co_3O_4 thin films

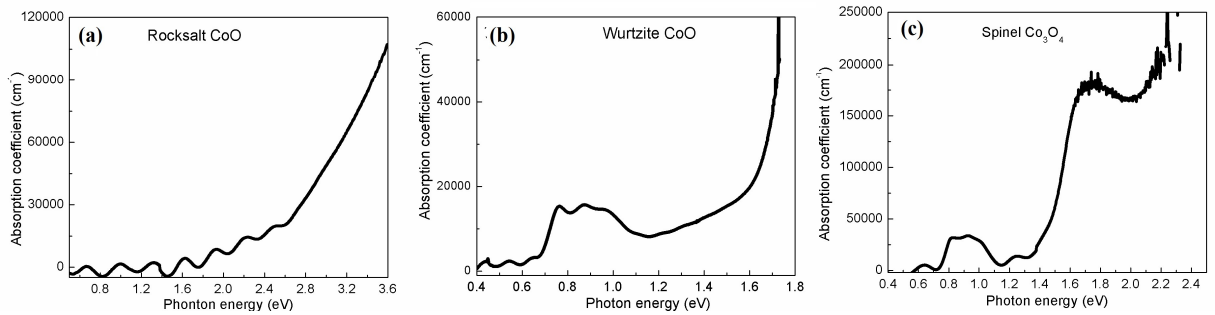

Fig. S6 Optical absorption spectra of rocksalt CoO (a), wurtzite CoO (b), and spinel Co_3O_4 (c) thin films.

Absorption spectra of rocksalt CoO, wurtzite CoO, and spinel Co_3O_4 thin films are presented in Fig. S6 for a side-by-side comparison. It is seen that the absorption spectrum of rocksalt CoO thin film does not show clear sub-gap absorption between 0.7 and 1.1 eV (see Fig. S6(a)). However, a significant sub-gap absorption is clearly observed in spinel Co_3O_4 thin film at the energy range of approximately 0.7 −1.1 eV (see Fig. S6(c)).